Tetrahydro[5]helicene-Based Nanoparticles for Structure-Dependent Cell Fluorescent Imaging

Meng Li, Li-Heng Feng, Hai-Yan Lu, Shu Wang,* and Chuan-Feng Chen**

Four new fluorescent dyes containing tetrahydro[5]helicene moiety characterized by three-primary emission colors (blue-green-red) are designed and synthesized, and their structures are characterized by NMR, MS, and single crystal X-ray crystallography. Organic nanoparticles based on the fluorescent dyes are then prepared by re-precipitation method, and their photophysical properties are investigated. These nanoparticles retain the strong emissions of the organic dyes, and multicolor nanoparticles were also prepared by simply tuning the ratios of the three-primary colors dyes. These organic nanoparticles exhibit low cytotoxicity, good photostability, and high quantum yields. Moreover, the nanoparticles can also be applied in the cell fluorescence imaging. Especially, it is interestingly found that the stained regions of these nanoparticles from membrane to cytoplasm for HeLa cells show obvious structure-dependent properties. This strategy provides a new perspective to fluorescence probe by molecular design for specific location imaging of living cells.

1. Introduction

Organic nanoparticles,[1–5] a kind of zero-dimensional self-assembled particles, have exhibited wide potential applications in chemical, biological and material sciences in the past decade.[6–8] Especially, organic nanoparticles assembled by π-conjugated polymers[9–13] have attracted much attention for their excellent photostability and low biological toxicity. Consequently, they have been successfully applied to various fields such as cells imaging, drug delivery and release, and disease diagnosis.[14–16] However, the uncertain molecular structures and complex components of the conjugated polymers could be unfavorable to the investigation of their structure-activity relationships, and also limit their practical applications. Hence, organic nanoparticles based on π-conjugated small molecules have aroused increasing interest in recent years,[17–21] such as Meijer and Schenning et al. reported a kind of organic nanoparticles containing fluorene-based oligomers in 2009, which showed the emissions covering the entire visible range.[22] Recently, Audebert et al. also obtained such kind of organic nanoparticles with white emission by tuning.[23] Up to date, such organic nanoparticles based on small molecule fluorescent dyes are still limited, in particular, few organic nanoparticles with multicolour emissions are reported. Moreover, although various organic fluorescent dyes have been reported,[24–29] few dyes with multicolor or full-color emissions based on the same skeleton were known.[30–33] Thus, the development of new small molecule dyes and their assembled organic nanoparticles is always one of most important subjects in this research area.

During the past decades, helicene derivatives[34,35] have received considerable attention for their wide potential applications in molecular machines, liquid crystals, and other research areas. Owing to their unique structures of polycyclic aromatic hydrocarbons, helicene derivatives could become a kind of important fluorescent dyes.[36] Unfortunately, few such organic dyes based on helicene derivatives have hitherto been reported.[37–40] Moreover, no organic nanoparticles assembled by helicene derivatives and their applications in cell imaging have been reported up to now. Herein, we report a new kind of tetrahydro[5]helicene based fluorescent dyes characterized by three-primary emission colors (blue-green-red), which can form a kind of homogeneous disperses of self-assembled organic nanoparticles with an average hydrodynamic diameters ranging from 39 nm to 86 nm. Similar to the photophysical properties of the dyes in THF solution, the organic nanoparticles also show strong emissions with three-primary colors in water. It is noted that multicolor nanoparticles could also be prepared by simply tuning the ratios of the three-primary colors dyes. Moreover, these organic nanoparticles with low cytotoxicity and excellent photostability can also be applied in the cell imaging.

M. Li, Prof. C.-F. Chen
Beijing National Laboratory for Molecular Sciences
Key Laboratory of Molecular Recognition and Function
Institute of Chemistry
Chinese Academy of Sciences
Beijing 100190, China
E-mail: cchen@iccas.ac.cn
Dr. L.-H. Feng, Prof. S. Wang
Key Laboratory of Organic Solids
Institute of Chemistry
Chinese Academy of Sciences
Beijing 100190, China
E-mail: wangshu@iccas.ac.cn
Prof. H.-Y. Lu
University of Chinese Academy of Sciences
Beijing 100049, China
E-mail: haiyanlu@ucas.ac.cn

DOI: 10.1002/adfm.201400199

© 2014 WILEY-VCH Verlag GmbH & Co. KGaA, Weinheim

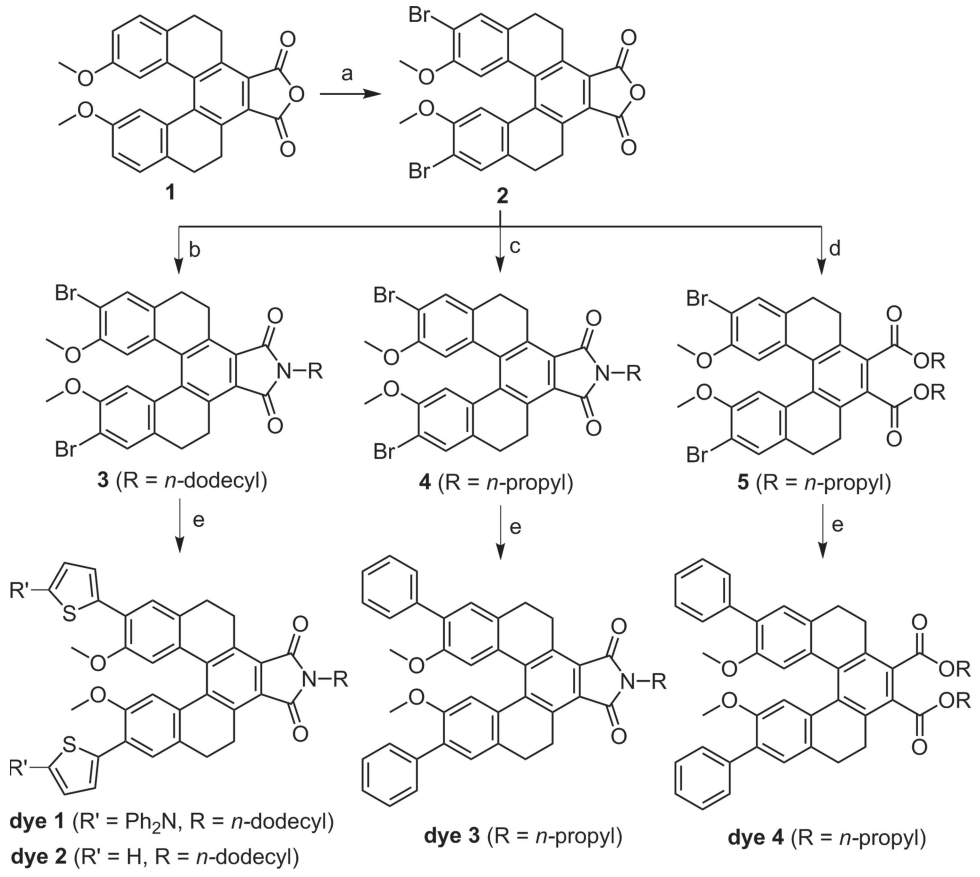

Scheme 1. Synthetic routes to **dyes 1–4**. Reagents and conditions: a) bromine (2 equiv), CH_2Cl_2, HOAc, r.t. 3 h, 80%; b) *n*-dodecyl amine (2.5 equiv), DMF, 90 °C, 24 h, 77%; c) *n*-propyl amine (5 equiv), DMF, 70 °C, 24 h, 70%; d) propanol, bromopropane, DBU, CH_3CN, reflux, 12 h, 73%; e) $Pd(PPh_3)_4$, arylboronic acid or arylborate (3 equiv), toluene/DMF, K_2CO_3, 90 °C, 12 h.

Interestingly, the stained regions of these nanoparticles from membrane to cytoplasm for HeLa cells show obvious structure-dependent properties. The results presented here will not only provide a feasible way for tetrahydro[5]helicenes as a fluorescence probe to biological applications, but also provide a kind multicolor nanoparticles and their structure-dependent cell imaging.

2. Results and Discussion

2.1. Synthesis and Structures of Dyes 1–4

The synthetic routes to **dyes 1–4** are depicted in **Scheme 1**. Starting from **1**,[36] compound **2** was conveniently obtained by the bromination reaction. Then by the reaction of **2** with *n*-dodecyl amine in DMF, dibromo-substituted lactim **3** was synthesized in 77% yield. Similarly, dibromo-substituted lactim **4** was obtained in 70% yield by the reaction of **2** and *n*-propylamine. With the lactims **3** and **4** in hand, **dye 1**, **dye 2**, and **dye 3** could be easily synthesized by Suzuki coupling reaction in 81, 83, and 79% yield, respectively. For **dye 4**, it could be conveniently synthesized by treatment of **2** with propanol in CH_3CN in the presence of bromopropane and 1,5-diazabicyclo[4.3.0]non-5-ene (DBU) followed by the reaction of dibromo-substituted ester **5** with phenylboronic acid. The chemical structures of the new compounds were all characterized by their ^1H NMR, ^{13}C NMR, and MALDI-TOF mass spectra. Fortunately, we also obtained a single crystal of **dye 3** suitable for X-ray diffraction analysis. The crystal structure of **dye 3** shows a non-planar structure with a torsion angle of 49.2° for C10-C16-C29-C28 (**Figure 1**a), and a dihedral angle of 45.2° between the aromatic rings A and B (Figure 1b). Moreover, by multiple C-H$\cdots\pi$ interactions, the molecules of **dye 3**

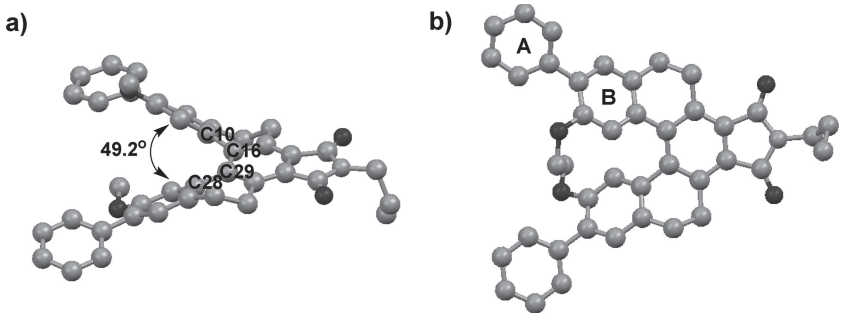

Figure 1. Crystal structure of **dye 3**. a) Top view, and b) side view.

© 2014 WILEY-VCH Verlag GmbH & Co. KGaA, Weinheim

could pack into a herringbone-like structure by different configuration arrangements alternately (Figure S2, Supporting Information), which could effectively prevent the quenching of its fluorescence in assembled conditions to some extent.

2.2. Preparation and Characterization of Organic Nanoparticles

With the dyes **1–4** in hand, we then prepared the dye nanoparticle (**DNP**) by a re-precipitation method (Figure S5, Supporting Information), in which organic solvent (THF, miscible with water) was added to water under ultrasonic without a surfactant. Consequently, the homogeneous disperses of **DNPs 1–4** in water were conveniently obtained by the self-assemblies of corresponding **dyes 1–4**, respectively. The DNPs were characterized by dynamic light scattering (DLS) and scanning electron microscopy (SEM). As shown in **Figure 2**, **DNP 1** displayed a spherical shape with a hydrodynamic diameter of 86 nm. Moreover, **DNP 1** also showed a negative zeta (ζ) potential value (–27.7 mV), which probably due to the O and N heteroatoms in **dye 1**. Similarly, it was found that the other three DNPs showed the average hydrodynamic diameters ranging from 39 nm to 86 nm, and the ζ potential values were found to be –19.4 mV, –17.3 mV, and –25.1 mV for **DNP 2**, **DNP 3**, and **DNP 4**, respectively (**Table 1**).

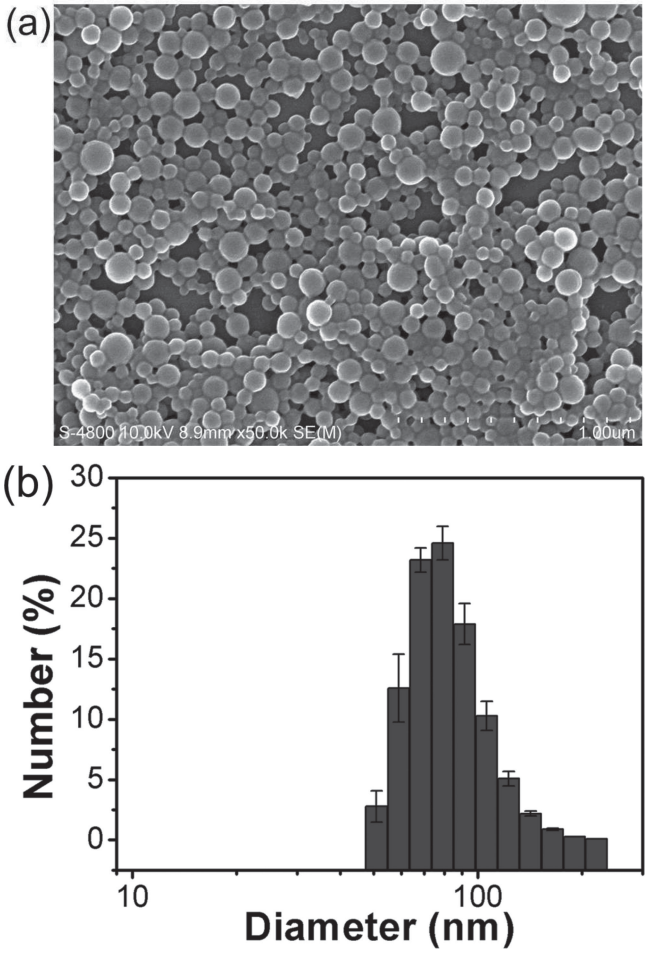

Figure 2. a) SEM image of **DNP 1**, and b) its hydrodynamic diameter measured by dynamic light scattering.

Table 1. The sizes and zeta potentials of DNPs.

	DNP 1	DNP 2	DNP 3	DNP 4
DLS [nm]	86	54	39	70
Zeta [mV]	–27.7	–19.4	–17.3	–25.1

2.3. Photophysical Properties of Dyes 1–4 and DNPs 1–4

The photophysical properties of **dyes 1–4** in THF solution were firstly investigated (Figure S3, Supporting Information), and the results were summarized in **Table 2**. The maximum absorption band of **dye 1** was observed at 431 nm, which was probably due to its large conjugated π system. The **dye 1** exhibits the maximum emission at 625 nm, which falls into the red-emitting region. Interestingly, owing to the strong intramolecular charge transfer in **dye 1**, the stokes shift is even up to 194 nm. Compared with **dye 1**, the maximum emission band of both **dye 2** and **dye 3** were respective hypsochromic shift to 519 nm and 483 nm, which may due to their weak intramolecular charge transfer. The fluorescence quantum yields of **dye 2** and **dye 3** were obviously enhanced to 52 and 51%, respectively. When the lactim moiety of **dyes 1–3** was replaced by two ester groups, both maximum absorption and emission bands of **dye 4** displayed further hypsochromic shift. Thus, it was found that all these dyes containing tetrahydro[5]helicene skeleton show large molar extinction coefficient and high quantum yield, and their fluorescence lifetimes fall into the nanosecond region (Figure S4, Supporting Information). Importantly, the emissions of the four dyes showed the three-primary colors (blue-green-red), which is helpful for the further realization of entire visible emission colors.

The photophysical properties of the corresponding nanoparticles (**DNPs 1–4**) were investigated in water. As shown in Table 2 and Figure S6, the assembled DNPs almost retain the

Table 2. Photophysical properties of **dyes 1–4** and **DNPs 1–4**.

Dyes and Nanoparticle	Absorption[a]		Fluorescence[a]		
	λ_{abs} [nm]	log(ε) [$M^{-1}cm^{-1}$]	λ_{em} [nm]	Φ_f[b] [%]	τ [ns]
dye 1	431	4.43	625	8	2.39
dye 2	399	4.37	519	52	5.99
dye 3	382	4.38	483	51	6.15
dye 4	352	4.26	445	29	3.25
DNP 1	460	4.11	625	4	
DNP 2	420	4.03	527	23	
DNP 3	390	4.00	502	27	
DNP 4	355	3.93	443	23	

[a]Photophysical properties of **dyes 1–4** were recorded in THF at room temperature ($c = 1.0 \times 10^{-5}$ M). Photophysical properties of **DNPs 1–4** were recorded in water at room temperature ($c = 2.5 \times 10^{-5}$ M); [b]Absolute fluorescence quantum yield, measured by Hamamatsu Photonics Quantaurus QY.

© 2014 WILEY-VCH Verlag GmbH & Co. KGaA, Weinheim

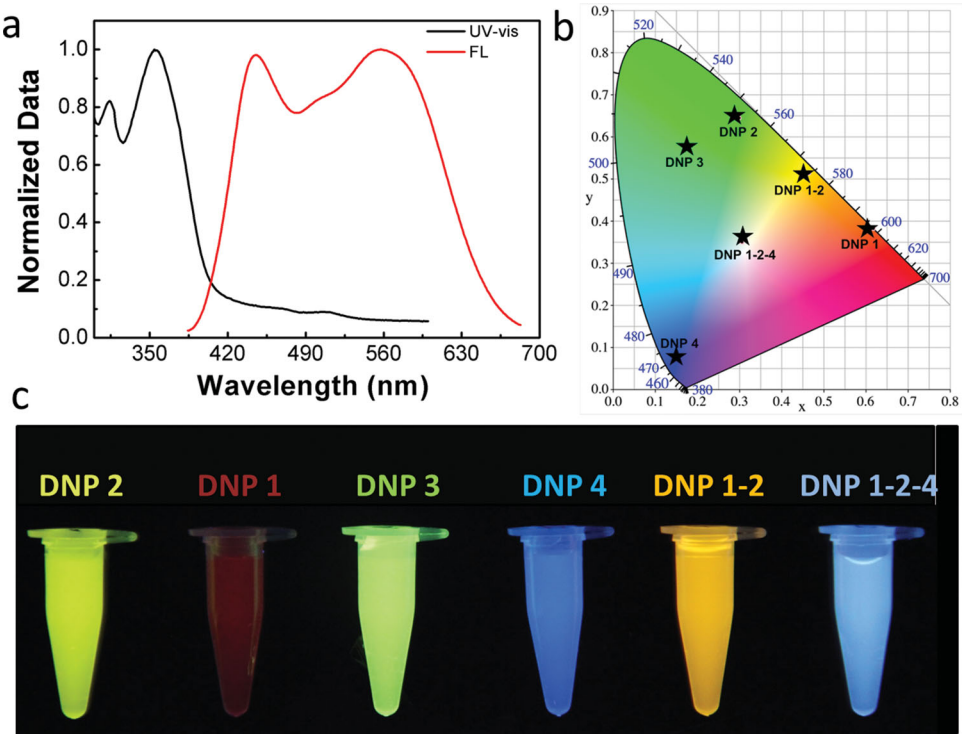

Figure 3. a) Absorption and emission spectra of **DNP 1–2–4** ($c = 2.5 \times 10^{-5}$ M); b) The 1931CIE coordinate diagram marked with coordinates corresponding to **DNP 1** (0.62, 0.38), **DNP 2** (0.30, 0.65), **DNP 3** (0.17, 0.57), **DNP 4** (0.15, 0.08), **DNP 1–2** (0.46, 0.51), **DNP 1–2–4** (0.30, 0.34) (emission spectra of the nanoparticles in water); c) The dispersion colors of DNPs under $\lambda_{ex} = 365$ nm excitation.

strong emissions of the organic dyes in solution from blue to azure and green to red color. Compared with **dyes 1–4** in THF, the maximum absorption of DNPs containing lactim moiety (**DNPs 1–3**) exhibit red-shift to some extent, while no significant change of was found for that of **DNP 4**. However, for the emission maxima of DNPs, only **DNP 2** and **DNP 3** show red-shift, while no significant changes were observed for those of **DNP 1** and **DNP 4**. Besides, all of these nanoparticles exhibit relatively good fluorescence quantum yield in water. The above results indicated that although the dyes exhibit the aggregation morphology, the corresponding DNPs still remain excellent photophysical properties.

2.4. Multicolor Regulation

The fluorescence emissions of **DNPs 1–4** exhibit the three-primary colors, which were confirmed by the 1931CIE coordinate diagram. As shown in **Figure 3**b, the CIE coordinates of the emission spectra of **DNPs 1–4** could be found at (0.62, 0.38), (0.30, 0.65), (0.17, 0.57), and (0.15, 0.08), respectively. In addition, the colors of the nanoparticle dispersions were also shown under light irradiation at 365 nm (Figure 3c). The multicolor nanoparticles covering the entire visible light region could be prepared by simply tuning the ratios of the three-primary colors dyes. For example, the orange-yellow **DNP 1–2** (580 nm, Figure S7, Supporting Information) could be obtained by mixing the **dye 1** and **dye 2** (30/1, mole) followed by re-precipitation method. Subsequently, **DNP 1–2–4** with the emission band covering 400–700 nm was also realized by adjusting the ratios of **dye 1**, **dye 2**, and **dye 4** (Figure 3a). The CIE coordinates of **DNP 1–2–4** is about (0.3, 0.34), which is desired value of white emission material. Noted that these multicolor DNPs display excellent photophysical properties (**Table 3**). Thus, the various colors or emission DNPs can be achieved by simply tuning the ratios of the three-primary colors dyes, which would provide full-color materials for biological, chemical and material fields.

2.5. Photostability and Cytotoxicity

The photostability and cytotoxicity of the nanoparticles are two critical factors for their applications in biological field. It was found that the fluorescence intensities of **DNPs 1–4** remain up to 60–80% of their original ones under continuous irradiation by a mercury lamp at 380 nm or 455 nm for 60s,

Table 3. Photophysical properties of **DNP 1–2** and **DNP 1–2–4**.

	λ_{abs} [a] [nm]	log(ε) [$M^{-1}cm^{-1}$]	λ_{em} [a] [nm]	Φ_f [b] [%]	DLS [c] [nm]	Zeta [d] [mV]
DNP 1–2	420	4.02	586	18.9	59	–27.8
DNP 1–2–4	355	3.98	400–700	–	137	–22.3

[a] Photophysical properties of **DNP 1–2** and **DNP 1–2–4** were recorded in aqueous solution at room temperature ($c = 2.5 \times 10^{-5}$ M); [b] Absolute fluorescence quantum yield, measured by Hamamatsu Photonics Quantaurus QY; [c] Hydrodynamic diameter measured by DLS; [d] Zeta(ζ)-potential.

© 2014 WILEY-VCH Verlag GmbH & Co. KGaA, Weinheim

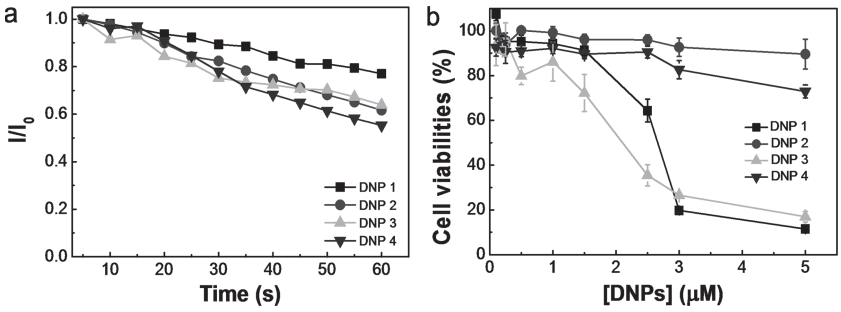

Figure 4. a) Photostability of nanoparticles (**DNPs 1–4**) upon irradiation at 380 nm or 455 nm under a mercury lamp, respectively; b) dose-response curve date for cell viability of Hela cell with nanoparticles (**DNPs 1–4**) by using a typical MTT assay.

respectively (**Figure 4**a), which show that these DNPs possess good photostability. Then, the 3-(4′,5′-dimethylthiazol-2′-yl)-2,5-diphenyl-2H-tetrazolium hydrobromide (MTT) assay was used to evaluate the cytotoxicity of nanoparticles, in which cell viability was determined by the conversion of MTT to formazan (Figure 4b). The **DNPs 1–4** exhibit lower cytotoxicity at the concentration below 2.0 μM. Although **DNP 2** and **DNP 3** display obvious cell cytotoxicity at the concentrations higher than 2.0 μM, it does not affect their cell imaging application, as the concentrations of DNPs in the cell imaging experiment do not exceed 2.0 μM.

2.6. In Vitro Cell Imaging

Biological application of DNPs for cells imaging was investigated by confocal laser scanning microscope (CLSM). The Hela cells were cultured with **DNP 2** at 37 °C for 12 h, and the fluorescence imaging was taken, where propidium iodide (PI) was used as a nucleus located dye. As shown in **Figures 5**a–d, both the membrane and cytoplasm regions of HeLa cells were stained by **DNP 2**. The imaging result was further verified by the 3D image of CLSM (Figure 5e). These results displays that **DNP 2** can be used as fluorescence probe for cell imaging.

Subsequently, the cells imaging in vitro using other three kinds of nanoparticles (**DNP 1**, **DNP 3**, and **DNP 4**) were also studied by CLSM (**Figure 6**). To our surprised, unlike **DNP 2**, those nanoparticles located on different and specific regions of Hela cells. As shown in Figure 6a, **DNP 1** (red emission) completely located on the membrane of HeLa cells, which hochest 33342 was used as a nucleus located dye. As shown in Figure 6b,c, however, the cytoplasm of HeLa cells were stained by **DNP 3** (green emission) and **DNP 4** (blue emission), where propidium iodide (PI) was used as a nucleus located dye. It is noted that the located regions of HeLa cells vary from the membrane to cytoplasm with the **DNPs 1–4**. The possible reason was attributed to the different substituents of tetrahydro[5]helicenes, which effected the cell phagocytosis process. The nanoparticles (**DNP 3** and **DNP 4**) assembled by tetrahydro[5]helicenes with short alkyl chain, have weaker interactions with the cell membrane, thereby these nanoparticles were easily phagocytized by the cells and stained the cytoplasm region by endocytosis action. However, the surface of **DNP 2** assembled by long chain of tetrahydro[5]helicenes possess stronger binding with the cell membrane by hydrophobic interactions. During the cell endocytosis processes, part of **DNP 2** was located in the membrane region except for its cytoplasm location. However, for **DNP 1**, besides the effect of long alkyl chain, the larger π-conjugated aryl substituted groups and tertiary amine units could also enhance the interaction of nanoparticles with cell membrane. Thus the **DNP 1** specifically located in the cell membrane. The stained regions of these nanoparticles from membrane to cytoplasm for HeLa cells showed obvious structure-dependent properties. This strategy provides a new perspective to fluorescence probe design for specific location imaging of living cells.

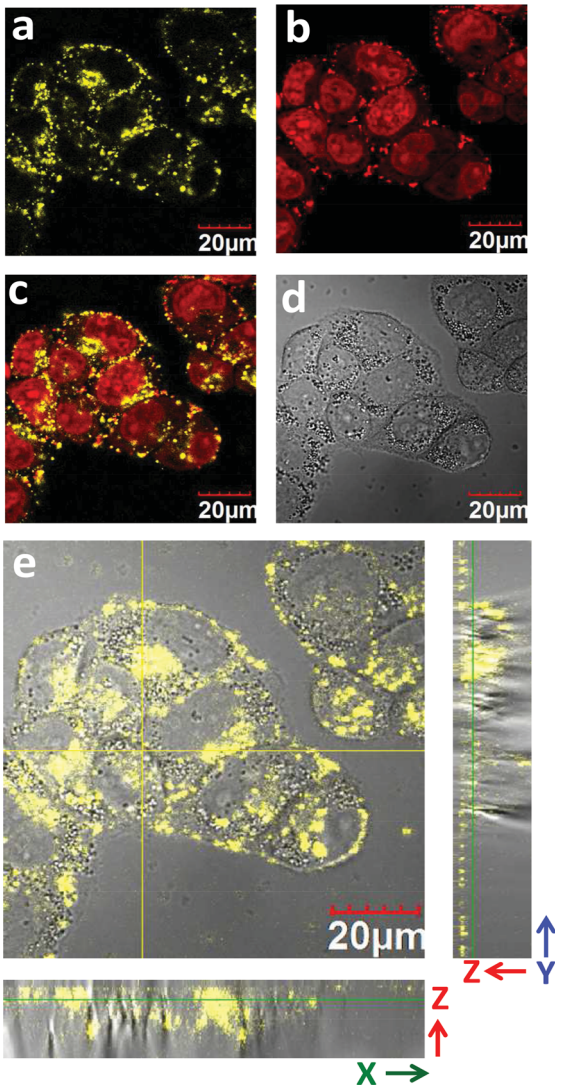

Figure 5. Fluorescence images of HeLa cells with **DNP 2**. a) CLSM image of **DNP 2**; b) CLSM image of PI; c) merged CLSM image of a and b; d) phase contrast image of Hela cells; e) merged 3D image of HeLa cells and **DNP 2**.

© 2014 WILEY-VCH Verlag GmbH & Co. KGaA, Weinheim

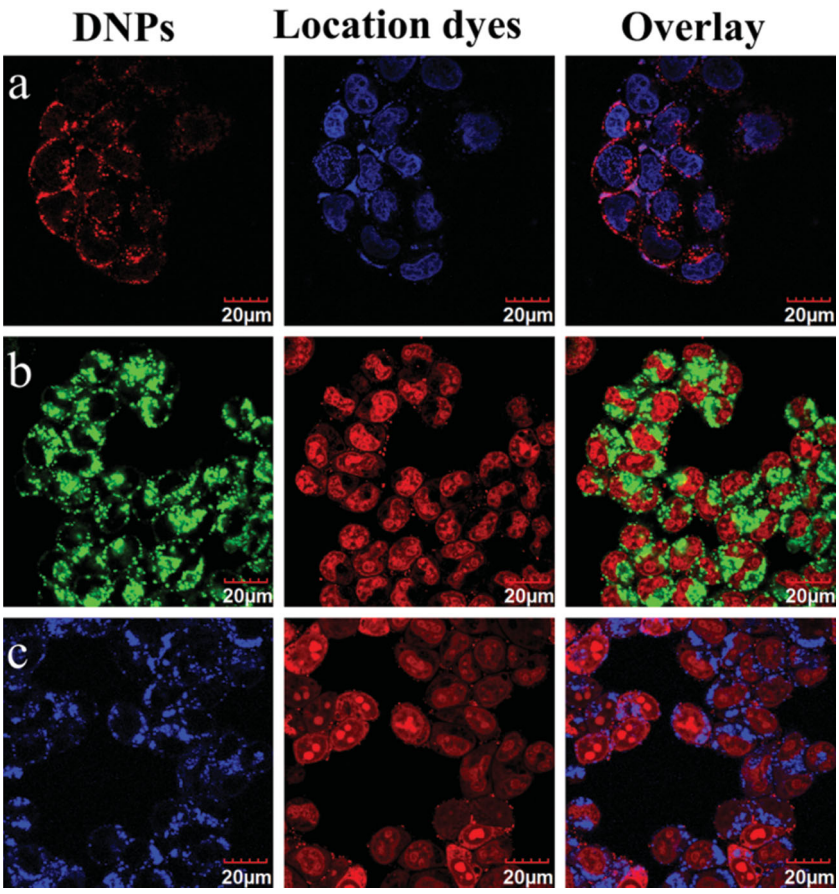

Figure 6. Fluorescence images of HeLa cells with a) **DNP 1**, b) **DNP 3**, and c) **DNP 4**. For **DNP 1**, the corresponding located dye was hochest 33342. For **DNP 3** and **DNP 4**, the corresponding located dyes were propidium iodide.

3. Conclusions

In conclusion, we have designed and synthesized four new fluorescent dyes based on the tetrahydro[5]helicene skeleton, and they exhibit three-primary emission colors (blue-green-red). By re-precipitating method, we successfully prepared four homogeneous dispersions of nanoparticles with hydrodynamic diameter of 39 to 86 nm. It was found that the nanoparticles in water retained the strong emissions of the organic dyes in THF solution. These organic nanoparticles exhibit low cytotoxicity in the biological tested conditions, excellent photostability and high fluorescence quantum yields. The multicolor nanoparticles covering the entire visible light region could be prepared by simply tuning the ratios of the three-primary colors dyes. Moreover, these organic nanoparticles could be applied in the cell fluorescence imaging. Especially, it was interestingly found that the stained regions of these organic nanoparticles from membrane to cytoplasm for HeLa cells showed obvious structure-dependent properties. The work presented here not only will show new applications of helicene derivatives as multicolor emission dyes, but also can provide a new perspective to fluorescence probe by molecular design for specific location imaging of living cells.

4. Experimental Section

Measurements: Melting points are uncorrected. ^{1}H NMR and ^{13}C NMR spectra were recorded with a DMX300 NMR at 298 K. MALDI-TOF mass spectra were determined with a BIFLEXIII mass spectrometer. HRMS mass spectra were measured in the ESI mode. All calculations were performed using the SHELXL97 and crystal structure crystallographic software packages. The UV-Vis absorption spectra were recorded on a JASCO V-550 spectrophotometer. Fluorescence spectra were measured on a Hitachi F-7000 fluorometer equipped with a Xenon lamp excitation source. Absolute fluorescence quantum yield, measured by Hamamatsu Absolute PL Quantum Yield Spectrometer C11347. Fluorescence lifetimes were measured by Quantaurus Tau C11367–11. Dynamic light scattering and Zeta(ζ)-potential experiments were carried out on Nano-ZS ZEN 3600 (Malvern Instruments, UK). SEM characterization was conducted by a Hitachi S-4300 scanning electron microscope. MTT analysis was performed on a microplate reader (BIO-TEK Synergy HT, USA) using the absorbance at 490 nm. Confocal laser scanning microscopy (CLSM) imagings were taken on a confocal laser scanning biological microscope (FV1000-IX81, Olympus, Japan).

Compound 2: To a solution of **1**[36] (20.6 g, 50 mmol) in CH_2Cl_2 (150 mL), bromine (16 g, 0.1 mol) in acetic acid (15 mL) was added slowly at room temperature. After the reaction mixture was stirred for another 3 hours, saturated aqueous Na_2SO_3 was added. The organic layer was concentrated in vacuo to give a crude product, which was further purified by recrystallization from CH_2Cl_2 to afford compound **2**[41] (22.7 g, 80%) as yellow solid. m. p.: 240–243 °C. ^{1}H NMR (300 MHz, $CDCl_3$, δ): 7.55 (s, 2H), 6.66 (s, 2H), 3.97 (d, J = 16.1 Hz, 2H), 3.39 (s, 6H), 2.93–2.80 (m, 4H), 2.64–2.50 (m, 2H). ^{13}C NMR (75 MHz, $CDCl_3$, δ): 163.3, 157.7, 141.0, 140.9, 133.5, 131.6, 129.1, 125.5, 116.2, 115.2, 55.3, 27.4, 24.8. HRMS (ESI) m/z calcd for $C_{26}H_{19}Br_2O_5$ $[M + H]^+$ 568.9594, found 568.9590.

Compound 3: A mixture of **2** (11.4 g, 20 mmol) and *n*-dodecyl amine (9.25 g, 50 mmol) in DMF (100 mL) was stirred for 24 h at 100 °C, and then cooled to room temperature. To the reaction mixture was added ethyl acetate (200 mL). The organic phase was washed with saturated brine (3 × 100 mL), dried over anhydrous $MgSO_4$, and then concentrated in *vacuo*. The residue was submitted to column chromatography with ethyl acetate and petroleum ether (1:5, v/v) as eluent to give **3** (11.37 g, 77%) as yellow solid. m. p.: 75–76 °C. ^{1}H NMR (300 MHz, $CDCl_3$, δ): 7.52 (s, 2H), 6.66 (s, 2H), 4.14–4.09 (m, 2H), 3.69–3.64 (m, 2H), 3.38 (s, 6H), 2.90–2.73 (m, 4H), 2.55–2.43 (m, 2H), 1.74–1.60 (m, 2H), 1.38–1.21 (m, 18H), 0.87 (t, J = 6.6 Hz, 3H). ^{13}C NMR (75 MHz, $CDCl_3$, δ): 168.8, 153.8, 138.4, 137.9, 133.2, 133.1, 132.6, 126.6, 114.5, 112.0, 56.0, 38.0, 32.0, 29.7, 29.7, 29.6, 29.5, 29.4, 28.7, 27.4, 27.0, 24.2, 22.8, 14.2. MALDI-TOF MS: *m/z* 737.2 $[M]^+$. HRMS (ESI) m/z calcd for $C_{38}H_{44}Br_2NO_4$ $[M + H]^+$ 736.1632, found 736.1623.

Compound 4: A mixture of **2** (11.4 g, 20 mmol) and *n*-propylamine (11.8 g, 0.1 mol) in DMF (100 mL) was stirred for 24 h at 70 °C, and then cooled to room temperature. Workup as described for **3** gave compound **4** (8.5 g, 70%) as yellow solid. m. p.: 271–272 °C. ^{1}H NMR (300 MHz, $CDCl_3$, δ): 7.52 (s, 2H), 6.66 (s, 2H), 4.18–4.07 (m, 2H), 3.71–3.60 (m, 2H), 3.38 (s, 6H), 2.90–2.75 (m, 4H), 2.55–2.43 (m, 2H), 1.78–1.65 (m, 2H), 0.97 (t, J = 7.4 Hz, 3H). ^{13}C NMR (75 MHz, $CDCl_3$, δ): 168.9, 153.8, 138.5, 137.9, 133.2, 133.1, 132.6, 126.6, 114.5, 112.1, 56.1, 39.6, 27.5,

© 2014 WILEY-VCH Verlag GmbH & Co. KGaA, Weinheim

24.3, 22.0, 11.5. MALDI-TOF MS: *m/z* 610.1 $[M+H]^+$. HRMS (ESI) *m/z* calcd for $C_{29}H_{26}Br_2NO_4$ $[M + H]^+$ 610.0223, found 610.0215.

Compound 5: A mixture of **2** (1.71 g, 3 mmol), 1-bromopropane (10 g), 1-propanol (10 g) and DBU (8 g) in acetonitrile (40 mL) was refluxed overnight, and then cooled to room temperature. Workup as described for **3** gave compound **5** (1.47 g, 73%) as white solid. m. p.: 84–85 °C. ^{1}H NMR (300 MHz, $CDCl_3$, δ): 7.47 (s, 2H), 6.57 (s, 2H), 4.34–4.18 (m, 4H), 3.36 (s, 6H), 3.09–2.98 (m, 2H), 2.85–2.73 (m, 4H), 2.70–2.56 (m, 2H), 1.82–1.70 (m, 4H), 1.01 (t, J = 7.4 Hz, 6H). ^{13}C NMR (75 MHz, $CDCl_3$, δ): 168.1, 153.8, 137.7, 134.8, 133.7, 132.8, 132.1, 130.5, 114.8, 111.4, 67.5, 56.1, 28.0, 27.7, 22.1, 10.7. MALDI-TOF MS: *m/z* 672.3 $[M]^+$. HRMS (ESI) *m/z* calcd for $C_{32}H_{33}Br_2O_6$ $[M + H]^+$ 671.0638, found 671.0644.

Dye 1: To a mixture of compound **3** (700 mg, 0.95 mmol), K_2CO_3 (1.31 g, 9.90 mmol), and 5-Ph_2N-2-thienylborate (1.07 g, 2.85 mmol) in DMF (30 mL) and toluene (20 mL) under argon atmosphere was added catalytic amount of $Pd(PPh_3)_4$ (5% mol). The resulting mixture was stirred for 12 hours at 90 °C under argon atmosphere, cooled to room temperature, and then added ethyl acetate (100 mL). The organic layer was washed with saturated brine (3 × 100 mL), dried over anhydrous $MgSO_4$, and then concentrated in *vacuo*. The residue was purified by column chromatography with ethyl acetate and petroleum ether (1:5, v/v) as eluent to give **dye 1** (828 mg, 81%) as red powder. m. p.: 117–118 °C. ^{1}H NMR (300 MHz, $CDCl_3$, δ): 7.49 (s, 2H), 7.36 (d, J = 4.0 Hz, 2H), 7.29–7.24 (m, 8H), 7.20–7.17 (m, 8H), 7.03 (t, J = 7.1 Hz, 4H), 6.82 (s, 2H), 6.65 (d, J = 4.0 Hz, 2H), 4.13 (d, J = 16.1 Hz, 2H), 3.71–3.62 (m, 2H), 3.38 (s, 6H), 2.93–2.77 (m, 4H), 2.59–2.44 (m, 2H), 1.72–1.65 (m, 2H), 1.32–1.25 (m, 18H), 0.87 (t, J = 6.6 Hz, 3H). ^{13}C NMR (75 MHz, $CDCl_3$, δ): 169.1, 153.4, 152.0, 149.0, 138.7, 138.2, 132.7, 132.4, 132.1, 129.3, 126.6, 126.2, 125.0, 123.7, 123.2, 123.0, 120.8, 114.1, 55.5, 38.0, 32.1, 29.8, 29.74, 29.65, 29.5, 29.4, 28.8, 27.8, 27.1, 24.5, 22.8, 14.3. MALDI-TOF MS: *m/z* 1078.5 $[M + H]^+$. HRMS (ESI) m/z calcd for $C_{70}H_{68}N_3O_4S_2$ $[M + H]^+$ 1078.46458, found 1078.46460.

Dye 2: To a mixture of **3** (700 mg, 0.95 mmol), K_2CO_3 (1.31 g, 9.90 mmol), and 2-thienylboronic acid (365 mg, 2.85 mmol) in DMF (30 mL) and toluene (20 mL) was added catalytic amount of $Pd(PPh_3)_4$ (5% mol). The resulting mixture was stirred for 12 hours at 90 °C under argon atmosphere, and then workup as described for **dye 1** gave **dye 2** (586 mg, 83%) as yellow powder. m. p.: 147–148 °C. ^{1}H NMR (300 MHz, $CDCl_3$, δ): 7.61 (s, 2H), 7.56–7.55(m, 2H), 7.35–7.33 (m, 2H), 7.11–7.08 (m, 2H), 6.86 (s, 2H), 4.19–4.13 (m, 2H), 3.70–3.65 (m, 2H), 3.40 (s, 6H), 3.00–2.81 (m, 4H), 2.61–2.49 (m, 2H), 1.74–1.63 (m, 2H), 1.33–1.26 (m, 18H), 0.87 (t, J = 6.6 Hz, 3H). ^{13}C NMR (75 MHz, $CDCl_3$, δ): 169.1, 153.5, 139.0, 138.7, 138.2, 132.9, 132.1, 127.4, 127.1, 126.3, 126.0, 125.9, 123.6, 114.3, 55.4, 38.0, 32.1, 29.77, 29.76, 29.74, 29.65, 29.5, 29.4, 28.8, 27.8, 27.1, 24.5, 22.8, 14.3. MALDI-TOF MS: *m/z* 743.3 $[M]^+$. HRMS (ESI) *m/z* calcd for $C_{46}H_{50}NO_4S_2$ $[M + H]^+$ 744.3176, found 744.3168.

Dye 3: To a mixture of **4** (603 mg, 0.99 mmol), K_2CO_3 (1.31 g, 9.9 mmol), and phenylboronic acid (362 mg, 2.97 mmol) in DMF (30 mL) and toluene (20 mL) was added catalytic amount of $Pd(PPh_3)_4$ (5% mol). The resulting mixture was stirred for 12 hours at 90 °C under argon atmosphere, and then workup as described for **dye 1** gave **dye 3** (473 mg, 79%) as yellow powder. m. p.: 267–268 °C. ^{1}H NMR (300 MHz, $CDCl_3$, δ): 7.54–7.51 (m, 4H), 7.44–7.39 (m, 4H), 7.37–7.27 (m, 4H), 6.87 (s, 2H), 4.19–4.14 (m, 2H), 3.70–3.64 (m, 2H), 3.33 (s, 6H), 2.95–2.83 (m, 4H), 2.64–2.52 (m, 2H), 1.80–1.68 (m, 2H), 0.99 (t, J = 7.4 Hz, 3H). ^{13}C NMR (75 MHz, $CDCl_3$, δ): 169.2, 154.3, 138.7, 138.5, 138.0, 133.2, 132.1, 131.0, 130.1, 129.4, 128.3, 127.4, 126.2, 114.1, 55.3, 39.5, 27.7, 24.5, 22.1, 11.6. MALDI-TOF MS: *m/z* 605.4 $[M]^+$. HRMS (ESI) m/z calcd for $C_{41}H_{36}NO_4$ $[M + H]^+$ 606.2639, found 606.2631.

Dye 4: To a mixture of compound **5** (60 mg, 0.09 mmol), K_2CO_3 (124 mg, 0.9 mmol), and phenylboronic acid (33 mg, 0.27 mmol) in DMF (15 mL) and toluene (10 mL) under argon atmosphere was added catalytic amount of $Pd(PPh_3)_4$ (5% mol). The resulting mixture was stirred for 12 hours at 90 °C under argon atmosphere, and then workup as described for **dye 1** gave **dye 4** (53 mg, 88%) as white solid. m. p.: 147–149 °C. ^{1}H NMR (300 MHz, $CDCl_3$, δ): 7.55–7.48 (m, 4H), 7.42–7.37 (m, 4H), 7.34–7.29 (m, 2H), 7.25 (s, 2H), 6.77 (s, 2H), 4.36–4.20 (m, 4H), 3.30 (s, 6H), 3.11–3.06 (m, 2H), 2.93–2.80 (m, 4H), 2.78–2.65 (m, 2H), 1.84–1.72 (m, 4H), 1.02 (t, J = 7.4 Hz, 6H). ^{13}C NMR (75 MHz, $CDCl_3$, δ): 168.5, 154.2, 138.2, 137.7, 135.4, 133.8, 131.6, 130.3, 130.1, 129.6, 129.4, 128.2, 127.2, 114.3, 67.4, 55.3, 28.3, 28.0, 22.1, 10.8. MALDI-TOF MS: *m/z* 666.3 $[M]^+$. HRMS (ESI) *m/z* calcd for $C_{44}H_{43}O_6$ $[M + H]^+$ 667.3054, found 667.30 60.

Preparation of DNPs 1–4: 125μL of the dyes in THF solution (1 mM) are diluted to 5 mL THF solutions, respectively. Then the solutions are rapidly injected into 12 mL water under the ultrasonic condition without any surfactants, After the ultrasound sustain for 3 minutes, the solutions are bubbled using Ar to remove the THF for 2 h, next, the remained solutions are heated to 110 °C with continual bubbling untill 5 mL of water is remained. Thus, the uniformly distributed nanoparticles are obtained.

Preparation of DNP 1–2 and DNP 1–2–4: Similar to the preparetion of **DNPs 1–4** by re-precipitating method, **DNP 1–2** was prepared from the mixture of different molar ratio of **dye 1**/**dye 2** (30/1) in 5 mL THF solution. Similarly, **DNP 1–2–4** was obtained from the mixture molar ratio of **dye 1**/**dye 2**/**dye 4** (1/0.2/100).

Cell Culture: Under a humidified atmosphere containing 5% CO_2, Hela cells were grown in DMEM medium containing 10% FBS routingly, then harvested for subculture using trypsin (0.05%, Gibco/Invitrogen) at 37 °C.

In Vitro Cell Viability Assay: The Hela cells were seeded in 96-well culture plates at a density of 8×10^3 cells per well and incubated 12 h for attachment. After incubated with DEME containing various concentrations of nanoparticles for 24 h respectively, the cells were washed with PBS twice and treated with 100 μL of 1 mg mL^{-1} MTT inPBS solution each well. Then the supernatant was discarded after incubation of 4 h at 37 °C, 100 μL DMSO was added per well. After shaking for five minutes, the purple formazan was recorded at 490 nm using microplate reader (BIO-TEK Synergy HT, USA).

Assay for Photostability of DNPs: The solution containing **DNPs** were dropped on a glass plate and covered with a coverslip. The samples were continuously irradiated by a mercury lamp (100 W) with a 380/30 nm excitation filter (for **DNP 3** and **DNP 4**) and a 455/70 nm excitation filter (for **DNP 1** and **DNP 2**). Fluorescence emission intensities of the samples were recorded with fluorescence microscopy (Olympus 1 × 71).

Cell Imaging: Hela cells were subculture onto a 35 mm × 35 mm Petri dish with a glass bottom, then allowed to grow for 24 h for attachment, after which 1 mL of DMEM medium containing 10% 25 μM nanoparticle was used to incubate the Hela cells at 37 °C for 24 h. the medium was replaced and phosphate-buffered saline (PBS, pH = 7.4) was used to wash the cells thrice. Then fresh medium with nuclear localization dye (PI or Hoechst) was added and incubated. After washing thrice with PBS, the images of the cells were recorded on confocal laser scanning microscopy.

Supporting Information

Supporting Information is available from the Wiley Online Library or from the author.

Acknowledgements

M.L. and L.-H.F. contributed equally to this work. The authors are grateful to the National Natural Science Foundation of China (21072220, 21272264, 91127009, TRR61), and the Major Research Plan of China (2011CB932501, 2011CB932302).

Received: January 20, 2014
Revised: February 8, 2014
Published online: March 24, 2014

© 2014 WILEY-VCH Verlag GmbH & Co. KGaA, Weinheim

[1] D.-E. Lee, H. Koo, I.-C. Sun, J. H. Ryu, K. Kim, I. C. Kwon, *Chem. Soc. Rev.* **2012**, *41*, 2656.
[2] D. H. M. Dam, J. H. Lee, P. N. Sisco, D. T. Co, M. Zhang, M. R. Wasielewski, T. W. Odom, *ACS Nano* **2012**, *6*, 3318.
[3] C. Wu, B. Bull, C. Szymanski, K. Christensen, J. McNeill, *ACS Nano* **2008**, *2*, 2415.
[4] K.-Y. Pu, K. Li, B. Liu, *Adv. Mater.* **2010**, *22*, 643.
[5] D. Maysinger, *Org. Biomol. Chem.* **2007**, *5*, 2335.
[6] E. Ahmed, S. W. Morton, P. T. Hammond, T. M. Swager, *Adv. Mater.* **2013**, *25*, 4504.
[7] M. Shen, X.-H. Zhu, A. J. Bard, *J. Am. Chem. Soc.* **2013**, *135*, 8868.
[8] J. Rauch, W. Kolch, S. Laurent, M. Mahmoudi, *Chem. Rev.* **2013**, *113*, 3391.
[9] C. Wu, C. Szymanski, Z. Cain, J. McNeill, *J. Am. Chem. Soc.* **2007**, *129*, 12904.
[10] J. Pecher, S. Mecking, *Chem. Rev.* **2010**, *110*, 6260.
[11] D. Tuncel, H. V. Demir, *Nanoscale* **2010**, *2*, 484.
[12] X. Feng, G. Yang, L. Liu, F. Lv, Q. Yang, S. Wang, D. Zhu, *Adv. Mater.* **2012**, *24*, 637.
[13] B. Bao, N. Tao, D. Yang, L. Yuwen, L. Weng, Q. Fan, W. Huang, L. Wang, *Chem. Commun.* **2013**, *49*, 10623.
[14] G. Wang, K.-Y. Pu, X. Zhang, K. Li, L. Wang, L. Cai, D. Ding, Y.-H. Lai, B. Liu, *Chem. Mater.* **2011**, *23*, 4428.
[15] L. Feng, C. Zhu, H. Yuan, L. Liu, F. Lv, S. Wang, *Chem. Soc. Rev.* **2013**, *42*, 6620.
[16] K. Petkau, A. Kaeser, I. Fischer, L. Brunsveld, A. P. H. J. Schenning, *J. Am. Chem. Soc.* **2011**, *133*, 17063.
[17] C. Vijayakumar, K. Sugiyasu, M. Takeuchi, *Chem. Sci.* **2011**, *2*, 291.
[18] Y. Koizumi, S. Seki, S. Tsukuda, S. Sakamoto, S. Tagawa, *J. Am. Chem. Soc.* **2006**, *128*, 9036.
[19] A. Jana, K. S. P. Devi, T. K. Maiti, N. D. P. Singh, *J. Am. Chem. Soc.* **2012**, *134*, 7656.
[20] K.-Y. Pu, K. Li, X. Zhang, B. Liu, *Adv. Mater.* **2010**, *22*, 4186.
[21] F. J. M. Hoeben, I. O. Shklyarevskiy, M. J. Pouderoijen, H. Engelkamp, A. P. H. J. Schenning, P. C. M. Christianen, J. C. Maan, E. W. Meijer, *Angew. Chem. Int. Ed.* **2006**, *45*, 1232.
[22] R. Abbel, R. van derWeegen, E. W. Meijer, A. P. H. J. Schenning, *Chem. Commun.* **2009**, 1697.
[23] J. Malinge, C. Allain, A. Brosseau, P. Audebert, *Angew. Chem. Int. Ed.* **2012**, *51*, 8534.
[24] Z. Yang, M. She, B. Yin, J. Cui, Y. Zhang, W. Sun, J. Li, Z. Shi, *J. Org. Chem.* **2011**, *77*, 1143.
[25] A. Loudet, K. Burgess, *Chem. Rev.* **2007**, *107*, 4891.
[26] A. Wakamiya, T. Murakami, S. Yamaguchi, *Chem. Sci.* **2013**, *4*, 1002.
[27] C. Kohl, T. Weil, J. Qu, K. Müllen, *Chem. Eur. J.* **2004**, *10*, 5297.
[28] D. Görl, X. Zhang, F. Würthner, *Angew. Chem. Int. Ed.* **2012**, *51*, 6328.
[29] C. Li, H. Wonneberger, *Adv. Mater.* **2012**, *24*, 613.
[30] J. E. Kwon, S. Park, S. Y. Park, *J. Am. Chem. Soc.* **2013**, *135*, 11239.
[31] C. Yuan, S. Saito, C. Camacho, S. Irle, I. Hisaki, S. Yamaguchi, *J. Am. Chem. Soc.* **2013**, *135*, 8842.
[32] A. Wakamiya, K. Mori, S. Yamaguchi, *Angew. Chem. Int. Ed.* **2007**, *46*, 4273.
[33] R. Bortolozzi, H. Ihmels, L. Thomas, M. Tian, G. Viola, *Chem. Eur. J.* **2013**, *19*, 8736.
[34] Y. Shen, C.-F. Chen, *Chem. Rev.* **2011**, *112*, 1463.
[35] M. Gingras, *Chem. Soc. Rev.* **2013**, *42*, 968.
[36] M. Li, H.-Y. Lu, R.-L. Liu, J.-D. Chen, C.-F. Chen, *J. Org. Chem.* **2012**, *77*, 3670.
[37] A. Rajapakse, K. S. Gates, *J. Org. Chem.* **2012**, *77*, 3531.
[38] H. Oyama, K. Nakano, T. Harada, R. Kuroda, M. Naito, K. Nobusawa, K. Nozaki, *Org. Lett.* **2013**, *15*, 2104.
[39] J. D. Chen, H.-Y. Lu, C.-F. Chen, *Chem. Eur. J.* **2010**, *16*, 11843.
[40] Z. Y. Wang, E. K. Todd, X. S. Meng, J. P. Gao, *J. Am. Chem. Soc.* **2005**, *127*, 11552.
[41] H. S. Blair, M. Crawford, J. M. Spence, V. R. Supanekar, *J. Chem. Soc.* **1960**, 3313.

© 2014 WILEY-VCH Verlag GmbH & Co. KGaA, Weinheim